

# Non-diffusive features of near-critical DTEM-turbulence in the presence of a subdominant diffusive transport channel

J. A. Mier<sup>1</sup>, R. Sánchez<sup>2</sup>, L. García<sup>1</sup> and D. Newman<sup>3</sup>

<sup>1</sup>*Universidad Carlos III de Madrid, Avda. de la Universidad 30, Leganés, Madrid, Spain*

<sup>2</sup>*Fusion Energy Division, Oak Ridge National Laboratory, Oak Ridge, Tennessee 37831-8071, USA*

<sup>3</sup>*Department of Physics, University of Alaska at Fairbanks, Fairbanks, Alaska 99775-5920, USA*

## 1 Introduction

A simple model of plasma turbulent transport via drift waves has been investigated in the light of ideas based on self-organized-criticality (SOC). This paradigm is based on the existence of the so-called SOC state, a fixed point of the dynamics, which exhibits spatial self-similarity and temporal persistence. The spatial and temporal characteristics of transport are coupled to each other: the lack of characteristic spatial scales is due to radial avalanche-like transport events with characteristic sizes only restricted by the system size. These avalanches depend on the instantaneous shape of the [density] profile which is continuously carved by past avalanches, through which memory effects remain active for as long as the system exists.

In this work we have examined how the properties of turbulent transport, in the context of dissipative-trapped-electron-mode (DTEM) turbulence with evolving mean profiles, change as a function of the relative strength of the subdominant diffusive channel to the turbulent one [1].

## 2 Model equation

The single-equation fluctuation model studied in this paper is a paradigm of plasma drift-wave transport [2] derived in the limit of long wavelengths for cylindrical geometry. In previous works, this model has been used to describe the dynamics of a plasma in a supercritical state. Now we use the same basic model to study the dynamics when the system stays in a near-critical state by letting the averaged density profile to evolve. Thus, an additional mechanism acts as a sink for fluctuations besides the direct turbulent cascade through large  $k$ 's: the averaged density profile relaxation.

## 3 Determination of transport exponents

Transport features can be characterized by measuring some characteristic exponents. These exponents can be obtained from the analysis of either time-series of some global quantity (such as the total flux or energy or some measure of local instability) or the features of tracer particle motion.

### 3.1 Turbulent activity

First, we concentrate on the profile dynamics and construct the time series of the global quantity,  $g(t)$ , which can be considered as a global measure of the turbulent activity in the system. It is constructed by evaluating, at each temporal step, at how many points of the numerical radial grid the local profile is unstable.

As an example, Figs. 1(a) and 1(b) show the form of  $g(t)$  for two extreme cases: no background diffusivity,  $D_0 = 0$ , and high diffusivity,  $D_0 = 10^{-9} a^2 \Omega_i$ . The number of unstable grid points is similar for both because, even with high values of  $D_0$ , transport is carried out mainly due to turbulent mechanisms. However, important changes are taking place in the dynamics as the background diffusivity is increased. This is related with the fact that  $g(t)$  seems to fluctuate over longer temporal scales for the highly diffusive case.

To quantify somewhat better the effect of  $D_0$  on the dynamics, we will discuss the  $R/S$  analysis and the power spectrum of the turbulent activity time-series.

- **R/S analysis.**-  $R/S$  analysis is a well-known technique to detect self-similarity of the turbulent activity signal as well as the range of scales over which self-similarity is present [3]. It simply measures how the range of the signal (defined as the maximum value minus its minimum value over some lapse of time  $\tau$ ), normalized to its variance, scales with the length of the signal. Self-similarity appears as a power-law dependence observed over a certain range of scales. The exponent  $H$  then reveals the existence of correlations ( $H > 1/2$ ), anti-correlations ( $H < 1/2$ ) or randomness ( $H = 1/2$ ).

For  $D_0 = 0$ , two distinct regions are found (see Fig. 2): a first region with  $H = 1$ , that extends up to  $\tau_H^g \sim (2 - 2.5) \times 10^3$  time steps and a second region with  $H \sim 0.8$  beyond that time that seems to extend up to the longest times in the simulation,  $(5 - 5.5) \times 10^5$  time steps. Correlations are thus strongly persistent as long as the simulation run. As diffusivity is increased, two observations can be made. First, that the time at which the transition between the  $H = 1$  and  $H < 1$  regions moves to shorter values. For instance, for  $D_0 = 10^{-9}$ , this transition happens at  $\tau_H^g \sim (3 - 5) \times 10^2$  time steps. The second observation is that the Hurst exponent of the tail region remains strongly persistent (see inset in Fig. 2) and still extends up for as long as the simulation lasts.

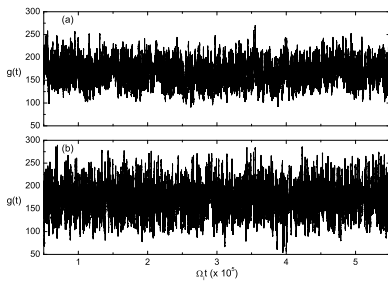


Figure 1: Time records of  $g(t)$ : (a) No external diffusion, (b) highly diffusive case.

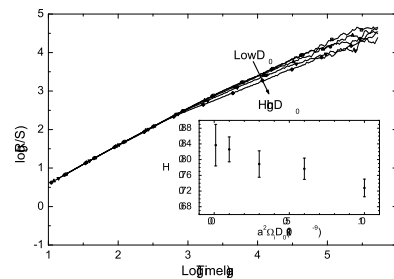


Figure 2:  $R/S$  analysis of  $g(t)$  for different values of  $D_0$ .

- **Power spectrum.**- In Fig. 3 the power spectra of the turbulent activity for a few

selected values of the diffusivity is presented. The first thing that is apparent is that several distinct power-law regions  $P(f) \propto f^{-\alpha}$  exist, as is typical in systems with self-similar dynamics of different character over different scale ranges. Their physical interpretation within the SOC context has been discussed elsewhere [4]. We will only focus on that related to the memory/persistence of the system. We find that all start at a frequency  $f_b^g \simeq (\tau_H^g)^{-1}$ , where  $\tau_H^g$  is the break point found in the R/S analysis. For frequencies larger than  $f_b^g$ , the information in the power-spectrum pertains to single avalanche dynamics: mostly their duration and temporal shape. For frequencies smaller than  $f_b$ , long-term correlations are found as  $f^{-\alpha}$  regions with  $0 < \alpha < 1$  for persistence and  $\alpha < 0$  for anti-persistence. For  $D_0 = 0$  a clear  $\alpha \simeq -1$  region is found, which was originally identified as the ultimate signature of SOC dynamics [5]. For  $D_0 > 0$ , the persistent region still exists but the exponent  $\alpha$  is reduced.

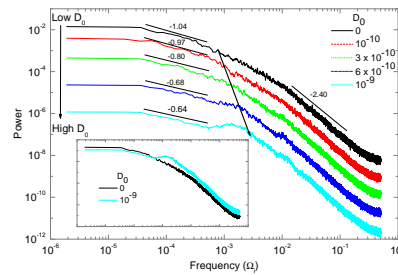


Figure 3: Power spectra of  $g(t)$  for different values of  $D_0$ .

### 3.2 Tracer particles: Lagrangian trajectories

We now investigate the transport properties induced by drift wave turbulence by characterizing the time evolution of particle tracers advected by the turbulence. We will only consider the advection due to the  $\mathbf{E} \times \mathbf{B}$  flow. Thus, the equation of motion of the tracers is,

$$\frac{d\mathbf{r}}{dt} = V_{\parallel}\mathbf{b} + \mathbf{V}_{\mathbf{E} \times \mathbf{B}} = V_0\mathbf{b} - \frac{1}{B^2}\nabla\tilde{\phi} \times \mathbf{B}, \quad (1)$$

where  $V_0$  is an arbitrary parallel velocity that can be varied to study its randomizing effect on the tracer Lagrangian trajectories.

#### - Continuous Time Random Walk-like diagnostics

When characterizing the transport properties of the tracers, we neglect the short range scale movements due to eddy trapping, which corresponds to fluctuation time scales. Instead, we concentrate on much longer times: times corresponding to jumps between eddies, flights, which extends roughly from the Lagrangian decorrelation time to the confinement time of the tracers. We define a flight as a radial displacement along which the velocity maintains the same sign.

Using the present definition of a flight, we can analyze the tracer orbits and compile the information through the probability distribution function (PDF) of the flights (see Fig. 4). To better identify the power law region we have joined positive and negative flights by taking the absolute value of the lasts, knowing that they are symmetric. The

decay index of the power-law region, which extends for almost a decade, is  $1 + \alpha \sim 1.7$ . The cutoff is due to finite system size effects.

### - Rescaled propagator

Another way of characterizing the transport properties is by inspecting the tracer propagators. That is, how an initially localized population of tracers evolves in time. Fig. 5 shows the rescaled propagator ( $t^H P$ ) at different times as function of the similarity variable  $r/t^H$ , with  $H = 0.75$ . A clear non-Gaussianity is apparent due to the power law exhibited over the interval  $\Delta r/t^H \in [2, 10] \times 10^{-2}$ . The decay index is now  $1 + \alpha \sim 1.6$ , consistent with the results obtained with the other diagnostic.

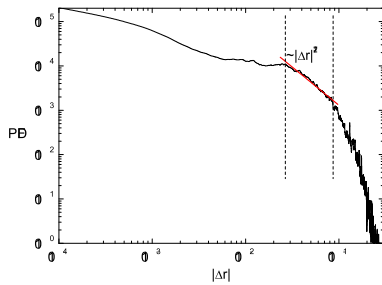


Figure 4: PDF of the flights.

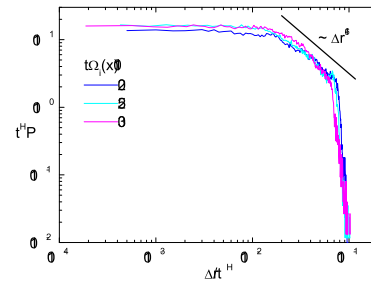


Figure 5: PDF of radial displacements.

## 4 Conclusions

The first conclusion of this work is that the existence of finite diffusivities imposed to the background averaged density profile does not necessarily invalidate the applicability of SOC-type models for plasma transport near a critical threshold. The reason is that the turbulent channel is always dominant, even for quite large diffusivities and thus memory effects, self-similarity and persistence remains present due to avalanche-like events in the system. This is true not only in the  $0^+$ -drive limit critical point but away from that. Our work also warns us of the danger of using the power-spectrum as a diagnostic tool for SOC. In particular, looking for a  $1/f$  region. Indeed, the correlated  $H$ 's are present even for smaller exponents in the power spectra [4].

The second conclusion refers to the tracer particle Lagrangian motion. The transport indexes obtained are in good agreement with those found for the turbulent activity. The system is non-local ( $\alpha \sim 0.6$ ), which is in agreement with the fact that avalanches are present in the system and non-Markovian ( $H \sim 0.75$ ) which again implies memory and persistence.

## References

- [1] J. A. Mier, L. Garcia and R. Sanchez, *Phys. Plasmas* **13**, 102308 (2006).
- [2] B. A. Carreras et al., *Phys. Fluids B* **4**, 3115 (1992).
- [3] H.E. Hurst, *Trans. Am. Soc. Civ. Eng.* **116**, 770 (1951).
- [4] R. Woodard et al., *Physica A* **373**, 215 (2007).
- [5] P. Bak, C. Tang and K. Wiesenfeld, *Phys. Rev. Lett.* **59**, 381 (1987).